

Hydroxytyrosol produced by engineered *Escherichia coli* strains activates Nrf2/HO-1 pathway: An *in vitro* and *in vivo* study

Yannis V Simos^{1*} , Stelios Zerikiotis^{1*}, Panagiotis Lekkas¹, Christianna Zachariou¹ , Maria Halabalaki², Filippos Ververidis^{3,4} , Emmanouil A Trantas^{3,4} , Konstantinos Tsamis¹, Dimitrios Peschos¹, Charalampos Angelidis⁵ and Patra Vezyraki¹

¹Laboratory of Physiology, Department of Medicine, School of Health Sciences, University of Ioannina, Ioannina 45110, Greece;

²Division of Pharmacognosy and Natural Products Chemistry, Department of Pharmacy, National and Kapodistrian University of Athens, Panepistimioupoli Zografou, Athens 11527, Greece; ³Laboratory of Biological and Biotechnological Applications, Department of Agriculture, School of Agricultural Sciences, Hellenic Mediterranean University, Estavromenos, Heraklion 71410, Crete, Greece; ⁴Agri-Food and Life Sciences Institute, Research Center of the Hellenic Mediterranean University, Estavromenos, Heraklion 71410, Crete, Greece; ⁵Department of Biology, Faculty of Medicine, School of Health Sciences, University of Ioannina, Ioannina 45110, Greece

*These authors contributed equally to this paper.

Corresponding author: Yannis V Simos. Email: isimos@uoi.gr

Impact statement

The numerous beneficial biological properties of hydroxytyrosol (HT) support its use in the production of nutraceuticals, agrochemicals, and cosmetics, as well as in the food industry. Extracting HT from natural sources is expensive, and chemical production suffers from low productivity. However, HT production through metabolically engineered microbial strains is an excellent eco-friendly alternative for producing highly pure HT. Our data indicate that HT, which is biotechnologically produced and purified with XAD-4 resin and fast centrifugal partition chromatography (FCPC), activates the Nrf2/HO-1 pathway and interacts differentially with the components of the endogenous antioxidant network. Moreover, repeated administration of 25 mg/kg body weight/day for 90 days showed no HT-related toxicity. These findings support the further exploitation of metabolic engineering to produce pure, low-cost, and biocompatible HT for large use scale in the industry.

Abstract

This study explores the biological effects of hydroxytyrosol (HT), produced by the metabolic engineering of *Escherichia coli*, in a series of *in vitro* and *in vivo* experiments. In particular, a metabolically engineered *Escherichia coli* strain capable of producing HT was constructed and utilized. HEK293 and HeLa cells were exposed to purified HT to determine non-toxic doses that can offer protection against oxidative stress (activation of Nrf2/HO-1 signaling pathway). Male CD-1 mice were orally supplemented with HT to evaluate (1) renal and hepatic toxicity, (2) endogenous system antioxidant response, and (3) activation of Nrf2/HO-1 system in the liver. HT protected cells from oxidative stress through the activation of Nrf2 regulatory network. Activation of Nrf2 signaling pathway was also observed in the hepatic tissue of the mice. HT supplementation was safe and produced differential effects on mice's endogenous antioxidant defense system. HT biosynthesized from genetically modified *Escherichia coli* strains is an alternative method to produce high-quality HT that exerts favorable effects in the regulation of the organism's response to oxidative stress. Nonetheless, further investigation of the multifactorial action of HT on the antioxidant network regulation is needed.

Keywords: Antioxidant activity, hydroxytyrosol, *in vivo*, metabolic synthesis, oxidative stress, supplementation, bioavailability

Experimental Biology and Medicine 2023; 248: 1598–1612. DOI: 10.1177/15353702231187647

Introduction

Hydroxytyrosol (HT) is a natural phenol of olive oil with a wide-ranging biological role. As a powerful antioxidant, HT scavenges free radicals, stimulates the synthesis and activity of endogenous antioxidant enzymes, and reduces lipid peroxidation.^{1,2} Moreover, HT exerts anti-inflammatory and anti-atherogenic effects.³ The disease-preventive profile of HT has been well documented in many studies of patients either supplemented with HT or consuming diets rich in olive oil.² It is not a coincidence that a panel of experts was

constituted by EFSA (European Food Safety Authority) to substantiate the health claims of HT and other olive oil polyphenols.⁴ These health-beneficial features of HT make it an ideal candidate for the development of food additives and supplements (nutraceuticals).

HT is derived as a hydrolysis product of more complex compounds such as oleuropein either during ripening of olive fruits or with time after olive oil production and storage.³ Many factors affect the HT content of olive oil, including olive variety, region microclimate, soil quality (factors that define oil quality)⁵ and the olive oil extraction process.⁶

Thus, the concentration of HT in olive oil vary, ranging from 0.2 ± 0.04 to 29.0 ± 0.42 mg/kg. Oleuropein, on the other hand, exists only in traces.⁷

HT can be isolated from olive products (olive oil or olive leaves) and can be produced by chemical synthesis or by microorganisms through the application of biotechnological approaches.⁸ However, the extraction of HT from natural sources is an expensive process. Although several chemical synthesis pathways leading to HT have been described from various precursor molecules (tyrosol, eugenol, catechol, DOPAC, homovanillyl alcohol, and so on), this methodology suffers from low productivity.⁸ Since HT recovery from olive mill wastewaters and other sources is inefficient, and chemical synthesis is expensive for industrial-scale production, the alternative HT production through metabolically engineered microbial strains in an industrial or semi-industrial type bioreactor is an excellent alternative.⁹ Such a biotechnological approach is an environmentally friendly method free from plant tissues that produce high levels of HT and is much easier and more economically purified.

Since HT is a biological molecule with wide-ranging biological uses, it has been included in a variety of products, including dietary supplements and food additives, raising the challenge to develop inexpensive and efficient manufacturing processes. Following this, HT has been produced by the enzymatic hydrolysis and high-temperature degradation of oleuropein, utilizing two cellulases with high β -glucosidase activity.¹⁰ Recently, novel nano-biocatalysts have been developed that can convert oleuropein to HT using immobilized β -glucosidase on porous carbon cuboids.¹¹ The immobilization of the enzyme β -glucosidase doubles the enzyme's ability to convert oleuropein to HT. HT has also been produced from wild type^{12,13} or metabolically engineered bacterial strains,^{14–16} though with varying efficiency and resource allocation. Especially for the metabolically engineered strains, varying genetic backgrounds, substrates, production processes or purification protocols have been utilized as alternative approaches.¹⁷

Here we report the *in vitro* and *in vivo* biological effects of purified HT biotechnologically produced from appropriate metabolically engineered *E. coli* strains, grown in a semi-industrial scale bioreactor. We further studied its pharmacological effects interacting or even reinforcing the antioxidant potential existing in the biological systems tested giving attention to the Nrf2/HO-1 signaling pathway, which is a complex regulatory mechanism that plays a pivotal role in oxidative stress diseases.

Materials and methods

Construction of *Escherichia coli* metabolically engineered strain

A metabolically engineered *Escherichia coli* strain capable of producing HT was constructed according to Trantas *et al.*⁹ A *Petroselinum crispum* DNA fragment of 1680 bp coding for an aromatic acetaldehyde synthase (AAS) was cloned from root complementary DNA (cDNA) utilizing the primer pair GTT ACC ATG GGC TCC ATC GAT AAT CTT ACT G / GGA TCC CTC AAA CCA GAG CAG AGA CAT GG with a Phusion DNA polymerase (Thermo Fisher Scientific).

It was then inserted into the pACYC Duet expression vector (Novagen, Merck Millipore), utilizing the *NcoI* and *BamHI* restriction enzymes to deliver the pACYC-PcAAS plasmid. The PcAAS gene sequence was experimentally confirmed by Sanger sequencing and was transferred into the BL21(DE3) *E. coli* strain to deliver the BL21-pACYC-PcAAS strain (abbreviated as B11T). The AAS activity in *in vitro* reactions was tested following a previously established protocol⁹ The whole construction scheme is shown in Figure 1.

HT production protocol from *E. coli* fed-batch growth in a semi-industrial-scale bioreactor and purification

In this work, HT was produced from the above-mentioned metabolically engineered *E. coli* B11T strain, grown in a fed-batch mode in a 50 L semi-industrial scale bioreactor (LP351, Bioengineering AG), where vessel temperature, agitation, pH, and aeration were tightly controlled. The bioreactor's vessel was filled with 28 L deionized water, the solid components of M9 minimal medium (6 g/L $\text{Na}_2\text{HPO}_4 \cdot 7\text{H}_2\text{O}$, 3 g/L KH_2PO_4 , 0.5 g/L NaCl, 1 g/L NH_4Cl , 120.4 mg/L MgSO_4 , and 11.1 mg/L CaCl_2 final concentrations), and was sterilized on site. After the sterilization, the temperature was set to 30°C and the medium was finalized with the addition of the rest of the components in liquid form, previously filter-sterilized (thiamine 10 nM, glucose 1%, chloramphenicol 34 mg/L final concentrations). The reaction was initiated with the inoculation of the medium with a 2 L overnight culture of B11T strain grown in Lysogeny Broth (yeast extract 5 g/L, tryptone 10 g/L, NaCl 10 g/L). B11T was let to grow until optical density reached $\text{OD}_{600} = 1$. Then the inducer reagent isopropyl β -D-1-thiogalactopyranoside (IPTG) was added to a final concentration of 200 μM to trigger transcription of the *lac operon* and thus induce protein expression of the AAS gene and let to grow for an additional 3 h. The precursor molecule, L-DOPA, was added to a final concentration of 4 mM and allowed to bio-transform to HT for an additional 12 h, with an expected 1:1 bio-transformation efficiency. By the end of the reaction, the B11T cells were separated from the medium by a high-speed tubular centrifuge (CEPA) and were frozen until purification. All analyses were performed in triplicate on a SCIEX UHPLC system consisting of an Exion LC model coupled with a QTRAP 4500 Triple quadrupole.

For HT purification, the methodology described by Xynos *et al.* was followed with some modifications. Briefly, XAD-4 resin was used for the selected adsorption of HT, while its recovery was achieved using isopropanol as an elution solvent. The final purification of HT took place using fast centrifugal partition chromatography (FCPC), leading to >95% purity.¹⁸

Cell lines

HEK293 (human embryonic kidney 293 cells, ATCC®CRL-1573) and HeLa (human cell line derived from cervical cancer, ATCC®CCL-2) cells were cultured in Dulbecco's modified eagle medium (high glucose for HEK293 and HeLa cells) supplemented with 10% (v/v) fetal bovine serum, 2 mM L-glutamine and 1% (v/v) penicillin-streptomycin (100 \times : 10,000 units/mL of penicillin and 10,000 $\mu\text{g}/\text{mL}$ streptomycin) in a humidified incubator (5% CO_2 , 95% air) at 37°C.

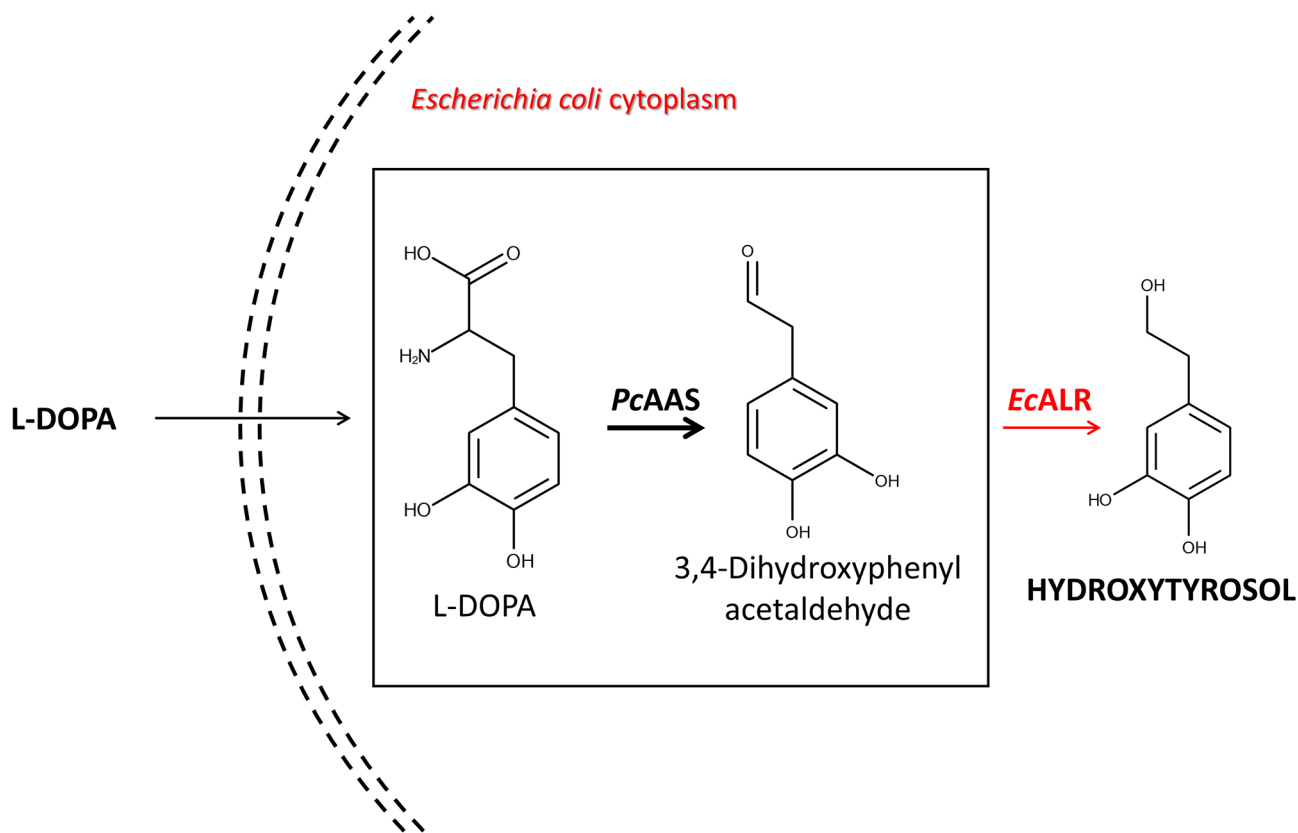


Figure 1. Hydroxytyrosol production scheme utilizing the activity of a heterologously expressed aromatic acetaldehyde synthase enzyme from *Petroselinum crispum* (PcAAS) and the activity of an endogenous aldehyde reductase (EcALR, red color). L-DOPA is externally supplemented to the cells, which is absorbed and transformed into HT.

Estimation of cell viability by MTT assay

The cells were plated in 96-well plates at a density of 5×10^3 cells/well and incubated for 24 hours before treatment with various concentrations of HT for 24 and 48 h. Cell viability was measured after incubation of each well with 50 μL of MTT (stock solution of 3 mg/mL) for 3 h. The medium was then removed, and the blue formazans were diluted with 200 μL of dimethyl sulfoxide (DMSO). Absorbance was determined at 570 nm (background absorbance measured at 690 nm) using a microplate spectrophotometer (Multiskan Spectrum, Thermo Fisher Scientific, Waltham, USA). All experiments were performed in triplicate.

Quantification of apoptosis by HT using flow cytometry

The cells were seeded into six-well plates at a density of (5×10^4) cells/well before the addition of HT. After 24 h incubation with HT, the supernatants and cells were collected (washed twice with ice-cold phosphate-buffered saline [PBS]), centrifuged, and cell pellets at a density of $10^5/100$ μL were suspended in a cold calcium-binding medium. Annexin V-FITC (5 μL) and PI (5 μL) double staining was used to quantify apoptosis. Samples remained for 15 min in the dark at room temperature. Analysis was performed on a fluorescence-activated cell sorting flow cytometer (Partec ML, Partec GmbH, Germany).

Determination of cellular reactive oxygen species levels

The cells were seeded for 24 h into six-well plates (at a density of 150×10^3 cells/well) with various HT concentrations (2.5–20 $\mu\text{g}/\text{mL}$). Cells were washed ($3 \times$ PBS) and treated with H_2O_2 (125 μM) and dichlorofluorescein diacetate (DCFH-DA) (2.5 μM) in Hanks' balanced salt solution for 15 min. Cells were then incubated with propidium iodide (PI; 1 $\mu\text{g}/\text{mL}$), placed on ice, and immediately analyzed on a fluorescence-activated cell sorting flow cytometer (Partec ML, Partec GmbH, Germany). For each sample, 10,000 events were measured.

In vivo effects of orally supplemented HT in CD1 mice

Male CD-1 mice, 2 months old, with a mean weight of approximately 30 ± 5 g, were used to evaluate the *in vivo* effects of orally supplemented HT. The mice were kept in cages (three animals per cage), at room temperature (25°C), under 12/12 h of light/darkness conditions. Mice chow (Viozois S.A., Animal Feed Company of Epirus, Greece) and water were provided *ad libitum*. Experiments were handled with humane care, following the European Union directive for the care and use of laboratory animals (EEC Directive 2010/63/EU; University of Ioannina, Approval no. 1657/23-2-2021).

The mice were randomly divided into three groups (10 animals per group): (1) the control group (CG), (2) the low

HT group (Low HT), and (3) the high HT group (High HT). HT was diluted in the drinking water for mice to achieve a concentration of 2.5 mg/kg for the Low HT group and 25 mg/kg for the High HT group per day. The supplementation period lasted 90 days.

Toxicological evaluation

All animals were euthanized using the approved by the Presidential Decree (56/30-4-2013) and EEC Directive (2010/63/EU) protocols at the end of the supplementation period and an autopsy was immediately performed. Mice's liver and kidneys were dissected and fixed in 10% buffered formalin. The samples were sent to the University Hospital of Ioannina for a histological evaluation by an experienced pathologist.

Effects of HT on catalase activity and glutathione levels

Blood was collected at the beginning (Day 0) and the end (Day 90) of the supplementation period. Blood samples were centrifuged at 3000 r/min for 20 min to separate the plasma from the red blood cells. All samples were stored at -80°C until use, to preserve long-term stability of the enzymes and other biochemical markers of the blood.^{19–21} The activity of catalase as well as glutathione (GSH) levels in mice plasma were determined utilizing spectrophotometry using the Megazyme Catalase Assay kit (Product Code: K-Catal) and the Sigma-Aldrich Assay kit (CS0260), respectively.

Detection of the Nrf2/Keap1 signaling pathway

For the detection of the protein expression of the key molecules of the Nrf2/Keap1 signaling pathway, analysis using Western blotting of both cell and tissue extracts was executed as previously described.²² Briefly, cells treated with different concentrations of HT and/or H_2O_2 , as well as control cells, were harvested, washed with PBS and then resuspended in RIPA Lysis buffer (50 mM Tris-HCl pH 7.5, 150 mM NaCl, 1% (w/v) Sodium deoxycholate, 0.1% (w/v) SDS, 1% (v/v) Triton-X-100, also containing 1 mM PMSF, 1 $\mu\text{g}/\text{mL}$ leupeptin and 1 $\mu\text{g}/\text{mL}$ pepstatin).

Hepatic tissue extracts from experimental animals administered with two different doses of HT (2.5 and 25 mg/kg body weight/day) for 90 days or water (control animals) were also prepared as previously described.²³ Hepatic tissues were homogenized with a tissue grinder with a mortar (Wheaton #358005) in Urea extraction buffer (125 mM Tris-HCl pH 6.8, 4 M Urea, 1 mM PMSF, 1 mM EDTA, 1 $\mu\text{g}/\text{mL}$ leupeptin, 0.5 $\mu\text{g}/\text{mL}$ pepstatin) at a rate of 10 μL for each mg of tissue. Then, total protein extracts were obtained after sonication for 30 s and centrifugation at 12,000 g for 5 min at 4°C .

In addition, nuclear protein samples were extracted from the hepatic tissues of the experimental animals or HeLa and HEK-293 cells with a Nuclear Extraction Kit (Abcam, ab113474) according to the manufacturer's protocol.

Cell and nuclear extract lysates were prepared, and then mixed with SDS (sodium dodecyl sulfate) Sample Buffer

(containing 62.5 mM Tris-HCl, 3% (w/v) SDS, 10% (v/v) glycerol, 5% (v/v) 2-mercaptoethanol, 0.01% (w/v) bromophenol blue) until a final concentration of $1\times$, and boiled for 5 min. After boiling, protein extracts (20 $\mu\text{g}/\text{sample}$) were analyzed with 10% SDS-polyacrylamide gel electrophoresis and subjected to Western blotting analysis using PVDF (polyvinylidene difluoride) membranes (Hybond P, Amersham). Then, blots were blocked in 10% dry fat milk in PBS for 1 h at room temperature, followed by overnight incubation at 4°C with the primary antibody in 3% bovine serum albumin (BSA) in PBS. After rinsing with Tris-buffered saline/Tween 20, blots were incubated with the peroxidase-conjugated secondary antibody (anti-mouse IgGk-HRP, dilution 1:5000, Santa Cruz Biotechnology, sc-516102 and anti-rabbit IgG-HRP, dilution, 1:3000, Pierce/Thermo Fisher Scientific, cat. no. 31460) for 1 h at room temperature. For the detection of the protein expression, the enhanced chemiluminescence method (Pierce, SuperSignal West Pico, Chemiluminescent Substrate CA 47079 – Clarity Western ECL Substrate, 500 ml #1705061) was used. The antibodies used were an anti-Nrf2 (dilution 1:1000, Rabbit mAb, Cell Signaling Technology, #12721) and an anti-HO-1 (1:1000, Rabbit mAb, Cell Signaling Technology, #43966) antibody. Also, anti- α -tubulin (1:5000, Mouse mAb, Santa Cruz Biotechnology, sc-5286) and anti-GAPDH (1:4000, Rabbit mAb, Cell Signaling Technology, #2118) antibodies were used as markers for the equal loading of samples.

Statistical analysis

Data are expressed as mean \pm SD. Statistically significant differences between data means were determined by one-way analysis of variance, and the Student's *t*-test was used for statistical evaluation of differences between groups, at different time intervals (SPSS version 20.0, Statistical Package for the Social Sciences software, SPSS, Chicago, IL, USA). The values of $p < 0.05$ were considered significant. The GraphPad Prism 8 software was used for creating the figures.

Results

Biotransformation of L-DOPA to HT

The metabolically engineered *E. coli* strain B11T was employed to bio-transform 114.4 g of L-DOPA (4.8 mM) into HT in four successive batches of 30 L cultivations. The precursor was fed into the bioreactor and after about 24 h, 67.52 g of HT (3.64 mM) was produced giving a yield of 76% (see Figure 2). The medium collected from four batches was frozen until purification.

HT exerted a potent cytotoxic effect

HT exerted a dose- but mainly time-dependent cytotoxicity against HEK293 cells. Cell viability remained well above 70% at the highest concentration (100 $\mu\text{g}/\text{mL}$) for the first 24 h of incubation. However, the prolongation of cell exposure to HT resulted in a steep decrease in cell survival as the doses of HT increased. Thus, a similar IC_{50} value to HeLa cells was estimated for HEK293 (21.9 ± 4.2 $\mu\text{g}/\text{mL}$ and 25.1 ± 8.5

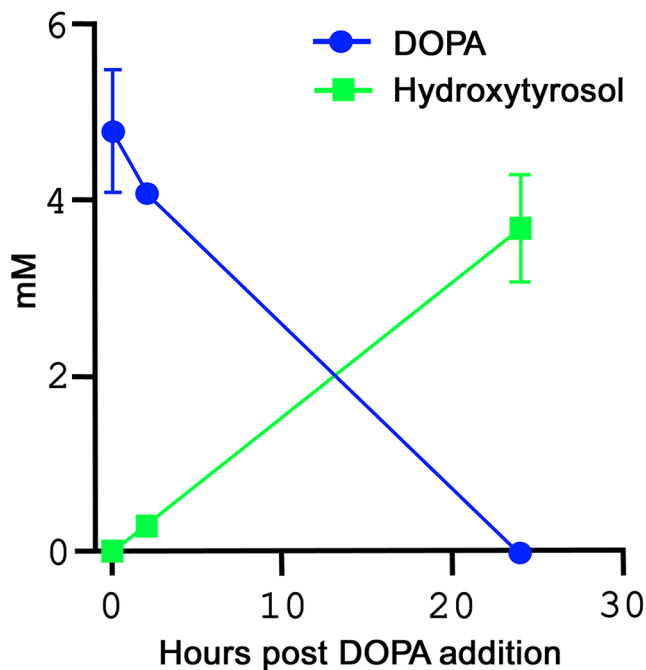


Figure 2. Time course presenting the biotransformation of L-DOPA into HT in a 30L bioreactor. On the vertical axis, the millimolar concentration of HT and L-DOPA are referred (mM).

$\mu\text{g}/\text{mL}$, respectively). The dose-dependent effect of HT on HeLa cells was evident after 24 h (IC_{50} $40.8 \pm 5.2 \mu\text{g}/\text{mL}$) of incubation whereas the extension of exposure to HT resulted in slightly lower rates of cell viability (IC_{50} $21.9 \pm 4.2 \mu\text{g}/\text{mL}$) (see Figure 3).

HT induced higher levels of apoptosis in cancer than in normal cells

HT induced apoptosis to a greater extent in HeLa cells than HEK293 (Figure 4(A) and (B)). The apoptotic effect was dose-dependent for both cell lines as shown in Figure 4(C) and (D). Initiation of apoptosis for HeLa cells was already visible at 24 h for doses higher than $20 \mu\text{g}/\text{mL}$. At 48 h, apoptosis was increased 9 \times for HeLa cells after exposure to $50 \mu\text{g}/\text{mL}$, compared to 3 \times for HEK293 cells (see Figure 4(B)).

HT inhibited hydrogen peroxide-induced reactive oxygen species formation

The ability of HT to scavenge intracellular reactive oxygen species (ROS) was investigated after staining the cells with the DCFH-DA fluorescent dye and utilizing flow cytometry. Exposure to hydrogen peroxide increased intracellular ROS formation by 30%. The preincubation of HeLa cells with HT resulted in a dose-dependent decrease in ROS formation. At $20 \mu\text{g}/\text{mL}$, HT not only managed to scavenge all the ROS generated by H_2O_2 but also ROS generated physiologically inside the cells; this was also seen for HEK293 cells at $5 \mu\text{g}/\text{mL}$ (135% reduction of the mean fluorescence intensity generated by H_2O_2). However, at higher doses (10 and $20 \mu\text{g}/\text{mL}$), HT completely abolished its ability to scavenge ROS (only a 10% reduction was recorded; see Figure 5).

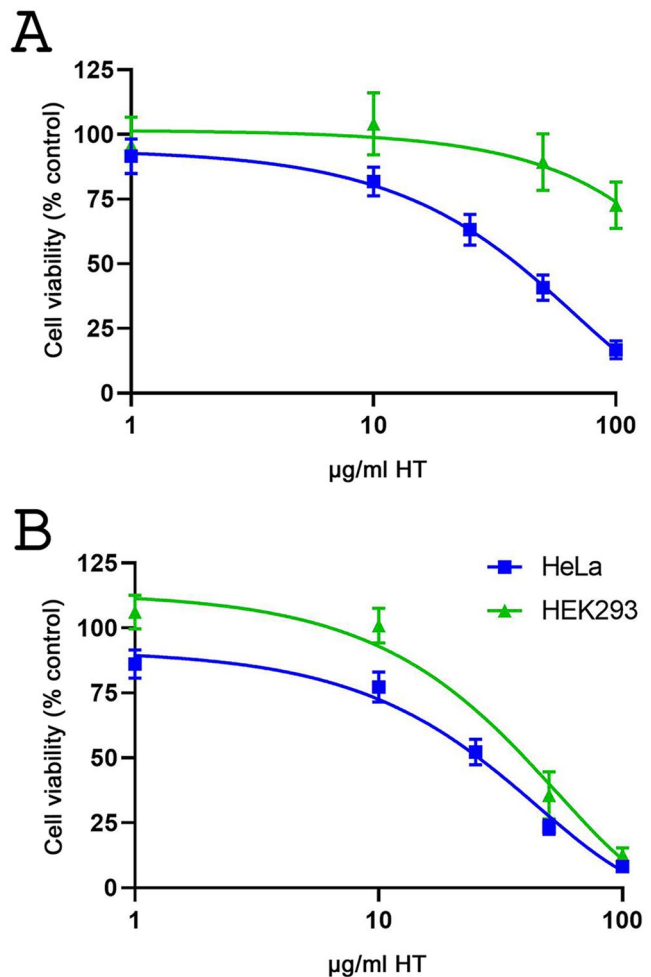


Figure 3. Cell viability of HeLa and HEK293 cells treated with 1–100 $\mu\text{g}/\text{mL}$ HT for (A) 24 and (B) 48 h. The results were normalized with the unexposed control. Data are presented as mean \pm standard deviation. All experiments were performed in triplicates.

Detection of the Keap1/Nrf2 signaling pathway after incubation with HT

Next, the identification of the mechanisms of the action exerted by HT, and the potential activation of the Keap1/Nrf2 signaling pathway were examined. For this purpose, the non-toxic concentrations of 5 and $10 \mu\text{g}/\text{mL}$ HT were initially chosen, and HeLa and HEK-293 cells were incubated for 24 and 48 h. For a better study of the antioxidant capacity and the protective effect of HT, cells were also exposed to a mild toxicity concentration of $250 \mu\text{M}$ H_2O_2 for 24 h after preincubation with 5 and $10 \mu\text{g}/\text{mL}$ HT for 24 and 48 h.

After treatment, SDS-PAGE electrophoresis and Western blot analysis showed that incubation of HeLa and HEK-293 cells with HT-induced protein expression of Nrf2 and HO-1 in both time intervals (24 and 48 h) used in our experimental protocol. Expression of Nrf2 and HO-1 seemed to increase after cell incubation only with $250 \mu\text{M}$ H_2O_2 for 24 h, and when cells were incubated with HT for 24 and 48 h, the increase in the expression of both proteins was even greater. Also, preincubation of both cell lines with HT before H_2O_2 exposure raised the expression of Nrf2 and HO-1 to a greater extent. According to our results, the effect of HT on

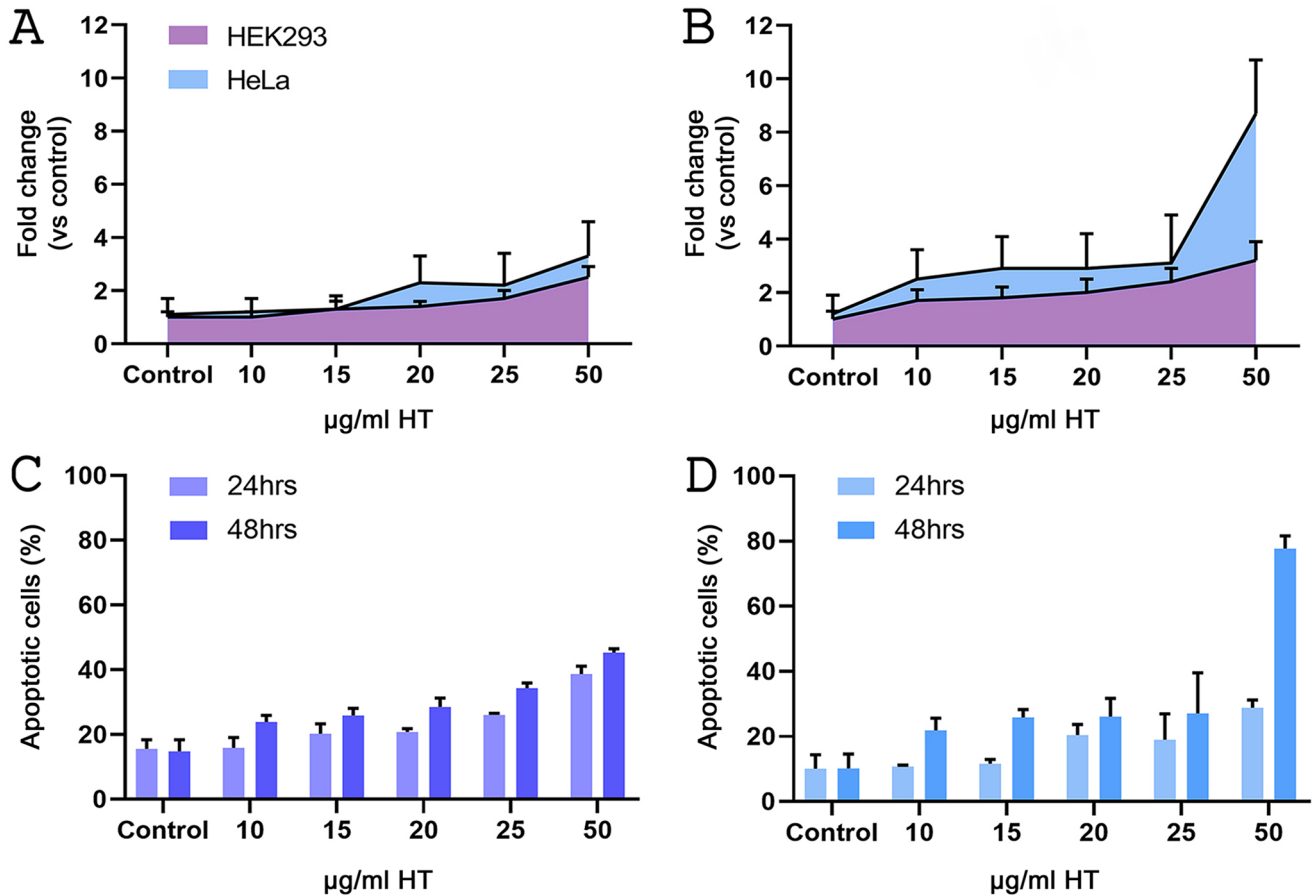


Figure 4. HT induces apoptosis in HeLa cells. (A) Initiation of apoptosis is more evident in HeLa than in HEK293 cells. (B) A steep increase in the apoptotic HeLa cell population at 50 $\mu\text{g/ml}$. (C) Dose-dependent effect of HT in HEK293 cells. (D) Dose- and time-dependent effect of HT in HeLa cells. Data are presented as mean \pm standard deviation. All experiments were performed in triplicates.

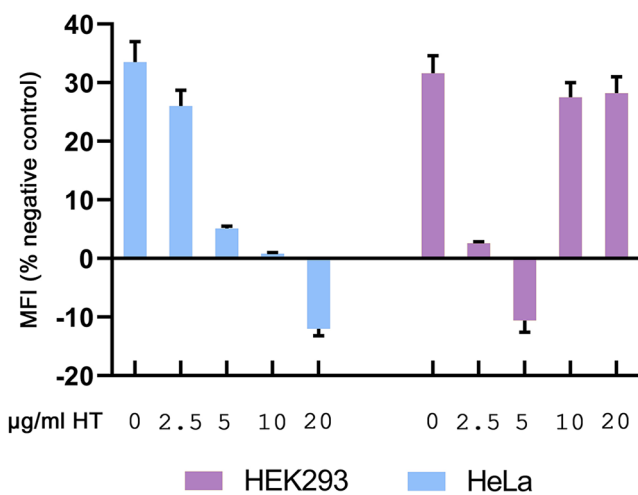


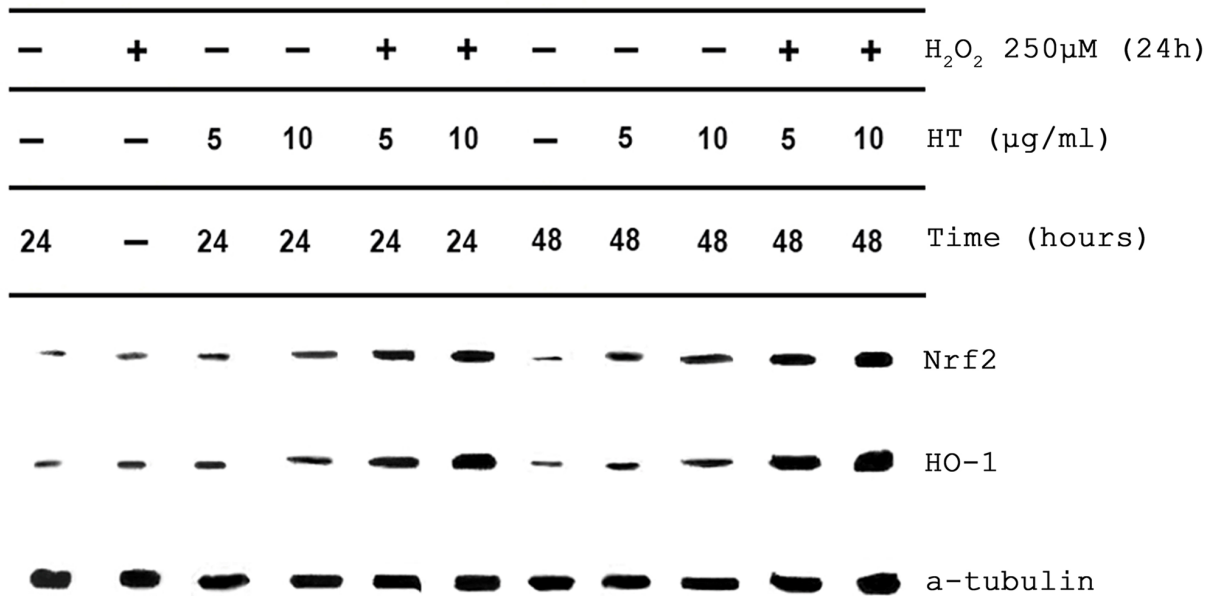
Figure 5. Reactive oxygen species (ROS) in HeLa and HEK293 cells measured by flow cytometry after staining with DCF-DA. Cells were pre-treated with 2.5–20 $\mu\text{g/ml}$ HT for 24 h and exposed to 125 μM H_2O_2 . Data are presented as mean \pm standard deviation. All experiments were performed in triplicates.

protein expression of Nrf2 and HO-1 seemed to be exerted in a dose- and time-dependent manner. The highest protein expression levels were observed at the concentration of

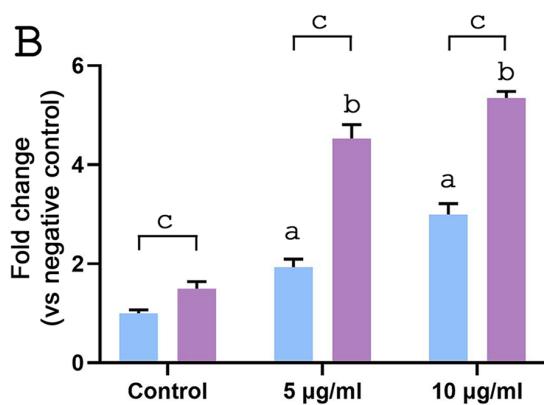
10 $\mu\text{g/ml}$ HT when administered to both cell lines for 24 and 48 h before exposure to H_2O_2 , as Nrf2 and HO-1 expression was increased more than four- to fivefold compared to control cells (see Figures 6 and 7). A comparison of the two cell lines showed that expression of Nrf2 and HO-1 was raised in HEK-293 cells in a comparable way to HeLa cells under the same incubation conditions. This increase was much more pronounced for Nrf2 protein levels, and it was not statistically significant in the HO-1 expression.

We then examined the potential HT-mediated translocation of Nrf2 to the nucleus. After extraction of nuclear lysates from HeLa and HEK-293 cells treated with 5 and 10 $\mu\text{g/ml}$ HT for 24 and 48 h or incubated with the same HT concentrations before exposure of cells to 250 μM H_2O_2 for 24 h, an induction of Nrf2 expression in the nucleus was observed for both concentrations of HT and the corresponding time intervals used. Treatment of both cell lines with HT increased Nrf2 expression in the nucleus, and this increase was more evident after incubation of cells to 5 and 10 $\mu\text{g/ml}$ HT for 24 and 48 h, followed by exposure to 250 μM H_2O_2 for 24 h. Nuclear Nrf2 expression levels were higher at the concentration of 10 $\mu\text{g/ml}$ HT for both time intervals when incubated either alone or before H_2O_2 . Under these conditions, Nrf2 expression increased about three to four and five to six times compared to the control cells in HeLa and HEK-293 cells, respectively (see Figure 8). Comparing the nuclear

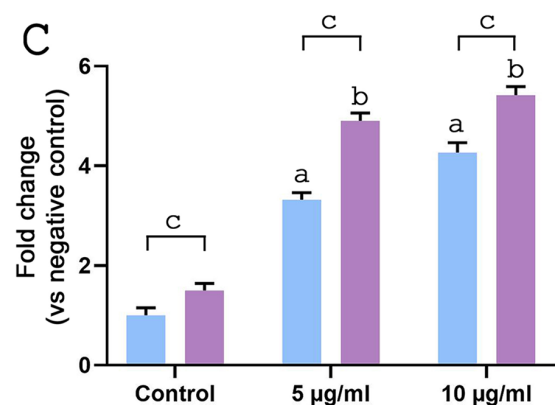
A



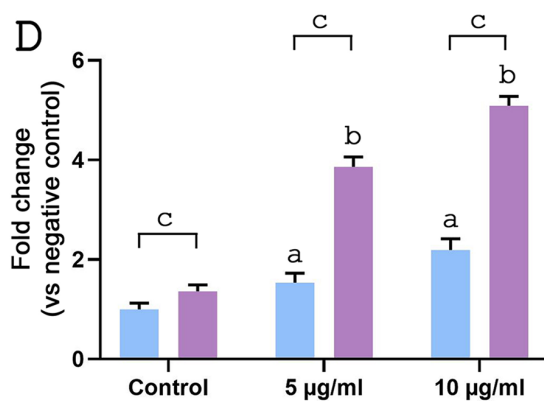
B



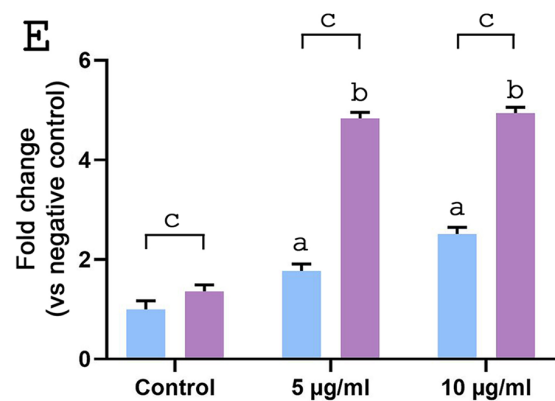
C



D



E



Legend: (-)H₂O₂ (blue bar), (+)H₂O₂ (purple bar)

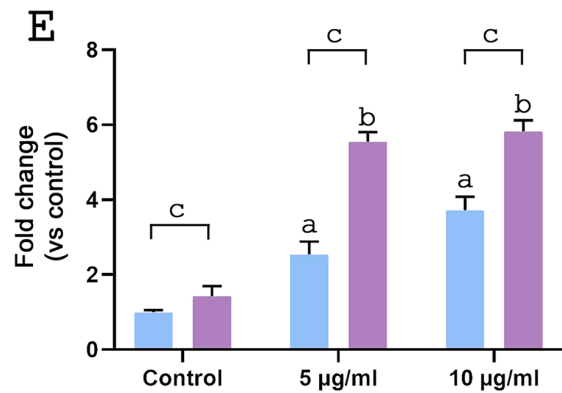
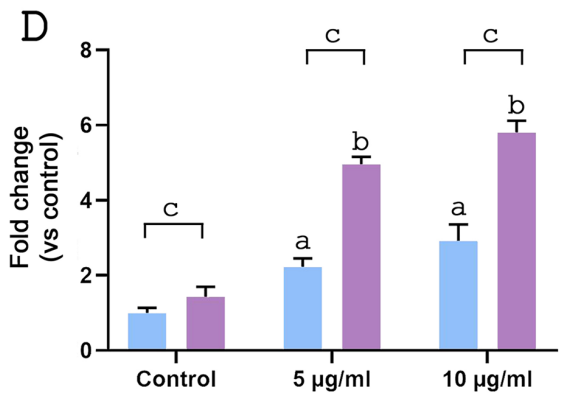
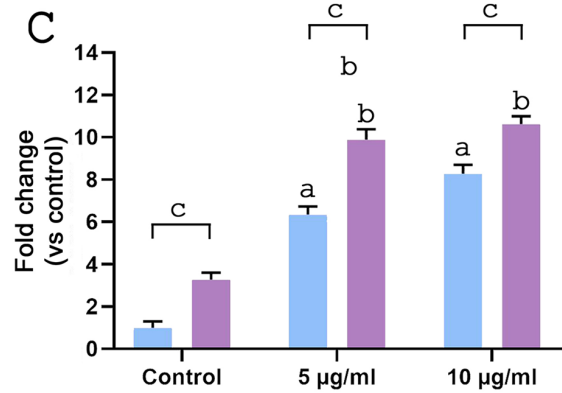
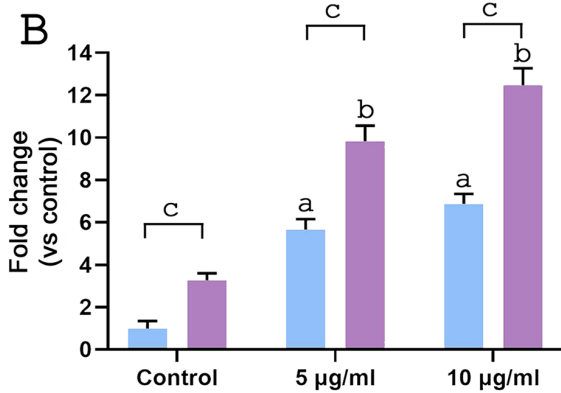
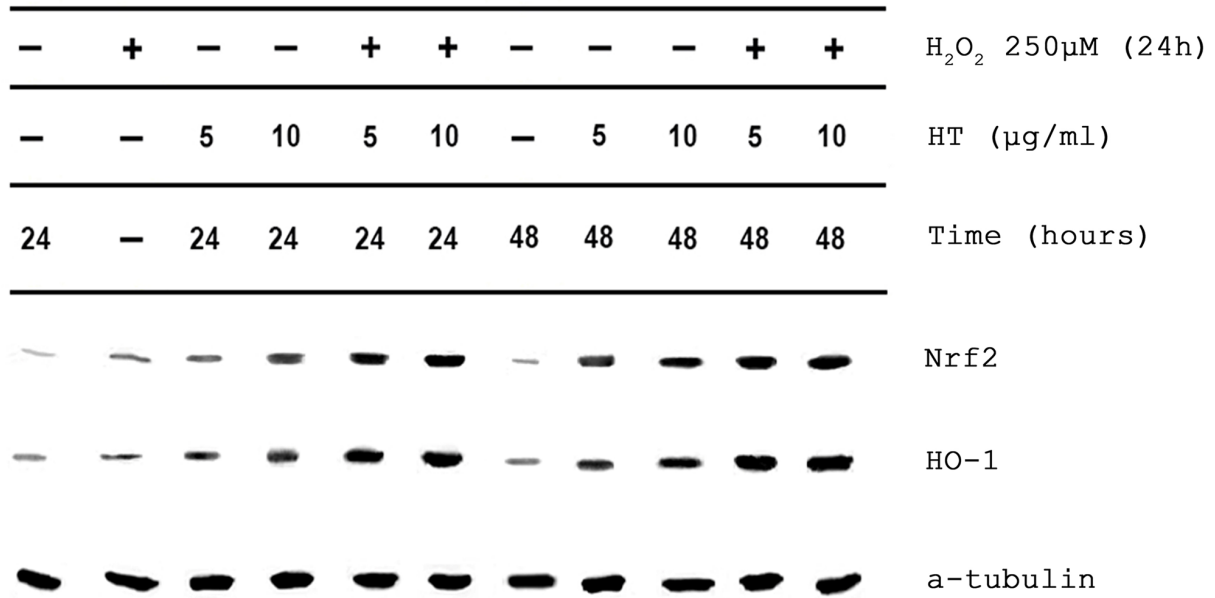
Figure 6. HT increases Nrf2 and HO-1 protein expression of HeLa cells. (A) Representative bands from total Nrf2 and HO-1 proteins. Pre-treated with HT for (B) 24 and (C) 48 h with/without exposure to H₂O₂ increased the expression of HO-1. Pre-treated with HT for (D) 24 and (E) 48 h with/without exposure to H₂O₂ also led to a similar Nrf2 increase in HO-1 expression.

^aStatistically significantly different from negative control.

^bStatistically significantly different from positive control.

^cStatistically significantly different between (-) and (+)-H₂O₂ at the same dose. Data are presented as mean ± standard deviation. All experiments were performed in triplicates.

A



Legend: (-) H₂O₂ (blue bars), (+) H₂O₂ (purple bars)

Figure 7. HT increases Nrf2 and HO-1 protein expression of HEK293 cells. (A) Representative bands from total Nrf2 and HO-1 proteins. Pre-treated with HT for (B) 24 and (C) 48 hours with/without exposure to H₂O₂ increased the expression of Nrf2. Pre-treated with HT for (D) 24 and (E) 48 h with/without exposure to H₂O₂ also increased HO-1 expression but at a lower rate than Nrf2.

^aStatistically significantly different from negative control.

^bStatistically significantly different from positive control.

^cStatistically significantly different between (-) and (+)-H₂O₂ at the same dose. Data are presented as mean ± standard deviation. All experiments were performed in triplicates.

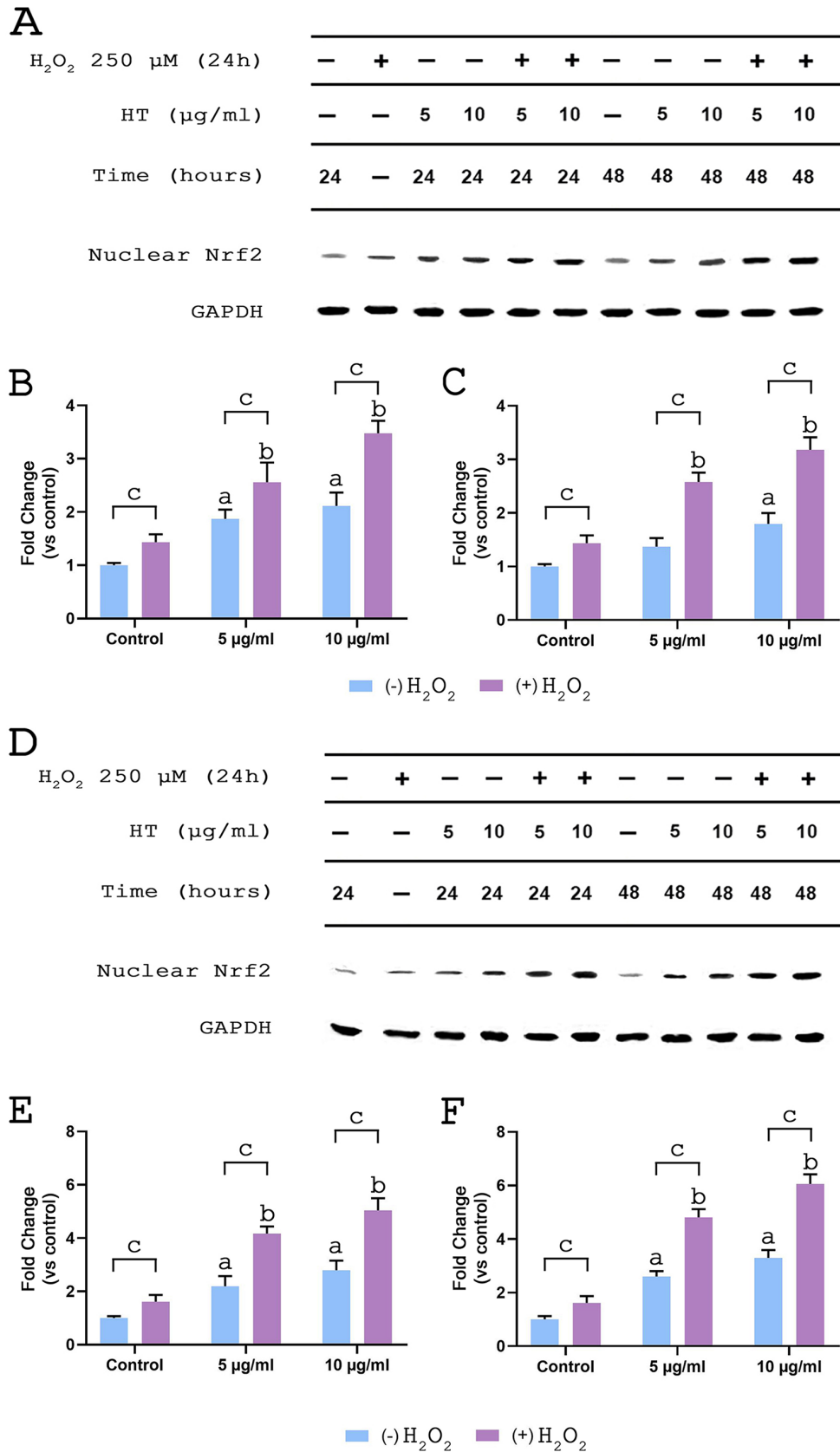


Figure 8. HT induces Nrf2 translocation into nuclei of (A, B, C) HeLa and (D, E, F) HEK293 cells. (A) Representative bands from nuclear Nrf2 in HeLa cells. Pre-treatment with HT for (B) 24 and (C) 48 h and exposure to H₂O₂ triggered the translocation and accumulation of Nrf2 in nuclei. (D) Representative bands from nuclear Nrf2 in HEK-293 cells. Pre-treatment with HT for (E) 24 and (F) 48 h and exposure to H₂O₂ triggered the translocation and accumulation of Nrf2 in nuclei at higher rates than in HeLa cells.

^aStatistically significantly different from negative control.

^bStatistically significantly different from positive control.

^cStatistically significantly different between (-) and (+)-H₂O₂ at the same dose. Data are presented as mean ± standard deviation. All experiments were performed in triplicates.

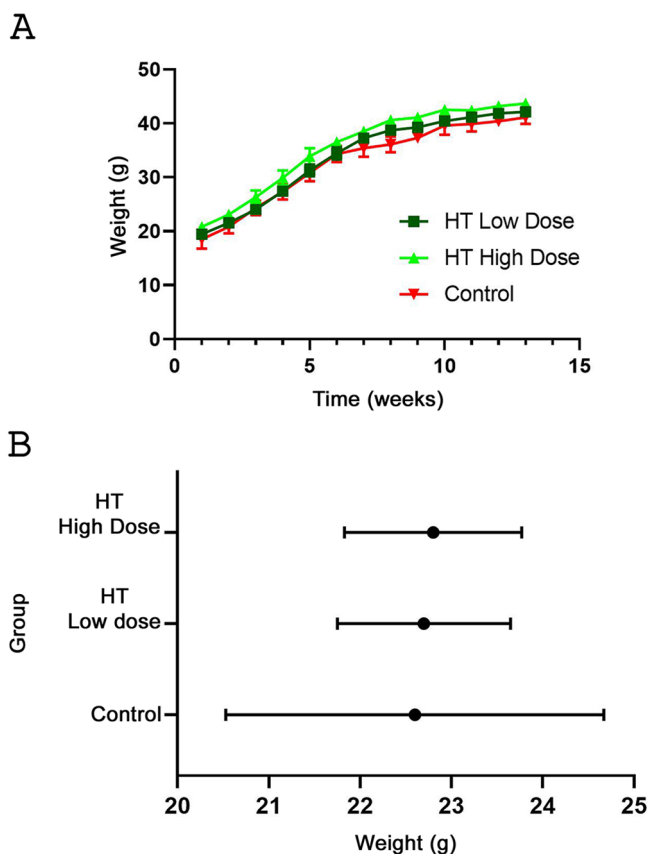


Figure 9. (A) Weight change of mice during supplementation period. (B) Mean weight gain in each group.

expression of Nrf2 between the two cell lines, a statistically significant rise in HEK-293 cells, compared to HeLa cells under the same treatment conditions, was observed.

Effect of HT on CD-1 mice body weight and liver and kidney toxicity

During supplementation, the Low and High HT groups' weight gain was similar to the control group as can be seen in Figure 9. The mice rapidly increased their weight until week 7; thenceforth, their weight was stabilized at around 40 g (see Figure 9(A)). The mean weight gain for each group was calculated at 23 g (see Figure 9(B)).

Evaluation of liver and kidney sections stained with H&E revealed no significant pathological features (see Figure 10). These results suggest that intake of HT for 90 days does not induce any specific toxicity in the liver and kidney organs of CD-1 mice at a dose of 25 mg/kg body weight/day.

Supplemental HT maintained catalase activity but decreased GSH levels in CD-1 mice

As shown in Figure 11(A), catalase activity in Low and High HT Groups remained constant throughout the supplementation period. Although a trend for an increase was noted in the High HT group with respect to catalase activity (12% increase), no statistically significant differences were detected.

Total GSH levels were similar in both groups and comparable to the control group at the beginning of the supplementation period. At the end of the study, a significant decrease ($p < 0.05$) was noted in both HT-supplemented groups. Interestingly GSH levels were 49% lower in the low-dose group and 15% in the high-dose group. The concentration of post-supplementation total GSH for the low-dose group was also statistically different (significantly lower) compared to the high-dose group ($p < 0.05$; see Figure 11(B)).

In vivo activation of the Keap1/Nrf2 signaling pathway after incubation with HT

In the next step of our research, we aimed to confirm the protective effect of HT on the hepatic tissues of experimental animals, and the identification of the potential pathway through which HT exerts its action. For this purpose, liver tissues from mice of all groups were isolated after administration with two different doses of HT (2.5 and 25 mg/kg body weight per day) or only with water (control mice) for 90 days. After total protein extraction from the hepatic tissues of the animals, protein cell extracts were analyzed with SDS-PAGE/Western blotting/ECL system, using specific antibodies against Nrf2 and HO-1. According to our results, an increased expression of Nrf2 protein in liver tissues from mice that were administered with both doses of HT compared to control mice was observed. Correspondingly, induction of the expression of HO-1 protein was observed in liver tissues of the group of mice that were administered with both the low and the high dose of HT compared to the control group of mice (see Figure 12(A) and (B)).

The increase in protein levels of both Nrf2 and HO-1 appeared to be more intense when mice were administered with the high dose of HT compared to the low dose, but this difference was not statistically significant. Administration with the low dose of HT to mice induced the Nrf2 and HO-1 expression about two to three times, while a high dose of HT caused a three- to fourfold increase in the protein levels of Nrf2 and HO-1 compared to the control group. In addition, HT seemed to induce Nrf2 expression in the nucleus of hepatic cells of the experimental animals after daily administration with the two HT doses for 90 days. A significant change was observed in the nuclear levels of Nrf2, with its expression being increased by approximately five and nine times in relation to the control group after administration with the low and the high dose, respectively. This difference between the two doses used in our experimental protocol concerning the nuclear Nrf2 expression was statistically significant ($p < 0.05$; see Figure 12(C) and (D)).

Discussion

Several *in vitro* and *in vivo* studies have shown that HT (and also its main precursor, oleuropein) have a wide spectrum of biological effects, which are characterized as beneficial for human health. The most important effects of HT are reported to be its anti-atherogenic, anticancer, antidiabetic, antithrombotic, and cardioprotective activity, and the efficient amelioration of cardiovascular and hepatic structure and function by HT has also been indicated.^{24,25} Based on

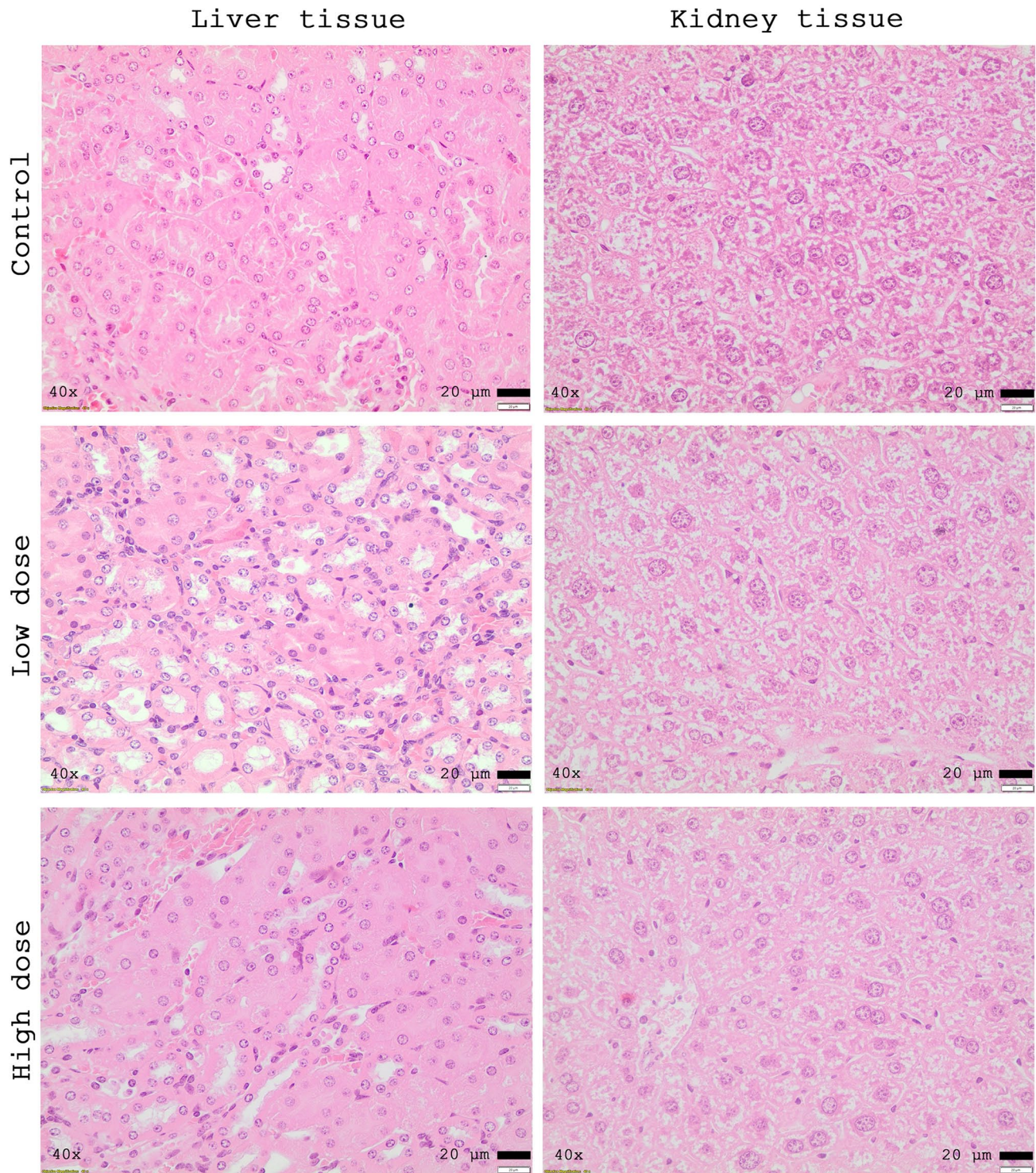


Figure 10. Representative histological images of liver and kidney tissue samples (40 \times magnification, scale bar 20 μ m). Tissue sections were stained with hematoxylin–eosin.

these properties, HT's potential clinical application is under investigation with several phase 2 or 3 clinical randomized trials aiming to verify that the findings from the *in vitro* experiments and animal studies can be translated into practical clinical recommendations²⁶ and HT supplementation could be widely used for the prevention and/or treatment of chronic diseases.

As we mentioned above, the extraction of HT from natural sources is an expensive process; thus, cheap and reliable methods that can produce high amounts of pure HT with minimal cost, will be of the utmost importance. Herein, we report for the first time that HT produced by a metabolic engineering strategy in *E. coli* strains increases the expression of Nrf2 with an analogous elevation in its nuclear translocation,

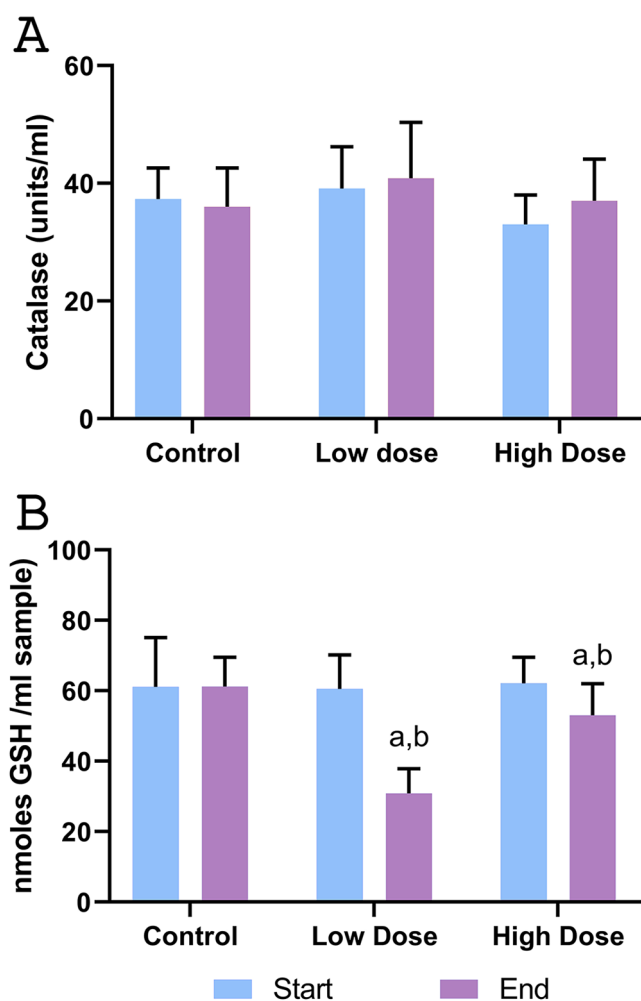


Figure 11. (A) Catalase activity in the plasma of CD1 mice before and after oral supplementation with 2.5 mg/kg/day (low dose) and 25 mg/kg/day (high dose) for 90 days. (B) Glutathione level in the plasma of CD1 mice before and after oral supplementation with 2.5 mg/kg/day (low dose) and 25 mg/kg/day (high dose) for 90 days.

^aStatistically significantly different from the Control Group.

^bStatistically significantly different from pre-supplementation levels within the same Group. Data are presented as mean \pm standard deviation. All experiments were performed in triplicates.

which results in an enhanced expression of HO-1. The Nrf2 role emerges in the regulation of oxidative stress caused by the excess production of ROS in the body cells. Total Nrf2 expression and nuclear translocation were more pronounced in HEK293 than in HeLa cells; however, HO-1 response was found to be similar in both cell lines. Exposure of cells to oxidative stress (H_2O_2 for 24 h) magnified the effect of HT on the expression of Nrf2 and subsequently on HO-1. Thus, HT could activate the Nrf2 pathway *in vitro*, playing a crucial role in the antioxidant defense, since it interacts with the antioxidant response element that controls oxidant homeostasis. However, according to the literature, the effect of HT on Nrf2 activity varies between studies and cells. A recent study showed that HT (50–150 μ M) reduces the expression of Nrf2 in human colorectal cancer cells (LS180) whereas a study from 2011 found no effect of HT on Nrf2 expression in

breast cancer cell lines MDA-MB231 and MCF7.²⁷ However, in the same study, HT increased the expression of Nrf2 in a normal epithelial cell line MCF10A.

Several cell studies have shown that substances with antioxidant properties may upregulate antioxidant defenses (activity of antioxidant enzymes) and also induce the death of cancer cells.^{27,28} The upregulation of antioxidant defenses is correlated with the production of ROS by HT; thus, HT acts mainly as a prooxidant in these cell studies and triggers an enhanced response from the antioxidant enzymes. On the contrary, HT antioxidant properties may also favor the balance of ROS levels in cells. Indeed, our results revealed that HT effectively reduces H_2O_2 -generated ROS at concentrations ranging up to 20 μ g/mL in HeLa cells. The same effect was seen in HEK293 cells but only at concentrations ranging up to 5 μ g/mL; at higher concentrations, the antioxidant ability of HT was completely abolished. Flow cytometry revealed that HeLa cells were more susceptible to the apoptotic effect of HT than HEK293 cells. Moreover, short-term exposure (24 h) to HT affected HeLa cell viability to a greater extent than that of HEK293 cells. In a recent study, it was shown that the deactivation of ROS by GPx3 regulates the MKP3-Erk-NF- κ B-cyclin B1 signal cascade, which suppresses the proliferation of lung cancer cells.²⁹ A potentially similar effect could be exerted by HT in HeLa cells; however, this assumption must be verified by further studies.

Boosting Nrf2 activity protects experimental animals from oxidative damage.³⁰ We demonstrated that supplementation of mice with HT caused a dose-dependent increase in the expression of Nrf2, its nuclear translocation and thus, HO-1 expression in liver tissue. Moreover, we noted a slight non-statistically significant increase in catalase activity of CD-1 mice supplemented with HT (low and high doses). HT can upregulate catalase activity *in vitro*³¹ and a recent clinical study showed that this upregulation of catalase is also feasible in the blood of volunteers 2 h after they were given phenol-rich extra virgin olive oil (that contained 9.4 mg of HT).³² Chronic supplementation of C57BL/6J male mice with 5 mg HT/day (for 12 weeks) did not improve hepatic catalase activity nor did it increase GSH hepatic content,³³ but acute (12 h after measurement) intraperitoneal injection of male BALB/c mice with 10 mg/kg HT (~0.25 mg per animal) significantly increased hepatic activity of catalase.³⁴

We also measured total GSH levels in mice blood. GSH is found in most tissues and protects cells (hepatocytes, erythrocytes, and so on) from toxic injury, which is caused by ROS and reactive nitrogen species (RNS).³⁵ Specifically, GSH scavenges ROS and RNS directly and indirectly through enzymatic reactions. Exposure of C2C12 myoblasts and EA.Hy926 endothelial cells to 10–25 μ g/mL HT for 24 h has been shown to increase GSH levels.³⁶ Numerous studies using experimental rodent models of diabetes demonstrated that administration of various doses of HT in different ways (orally, intraperitoneally, gavage) can effectively increase the activity of superoxide dismutase (SOD) and catalase in the liver, kidney, pancreas, and blood, and GSH concentration in the pancreas and liver.³⁷ Notably, a very steep decrease

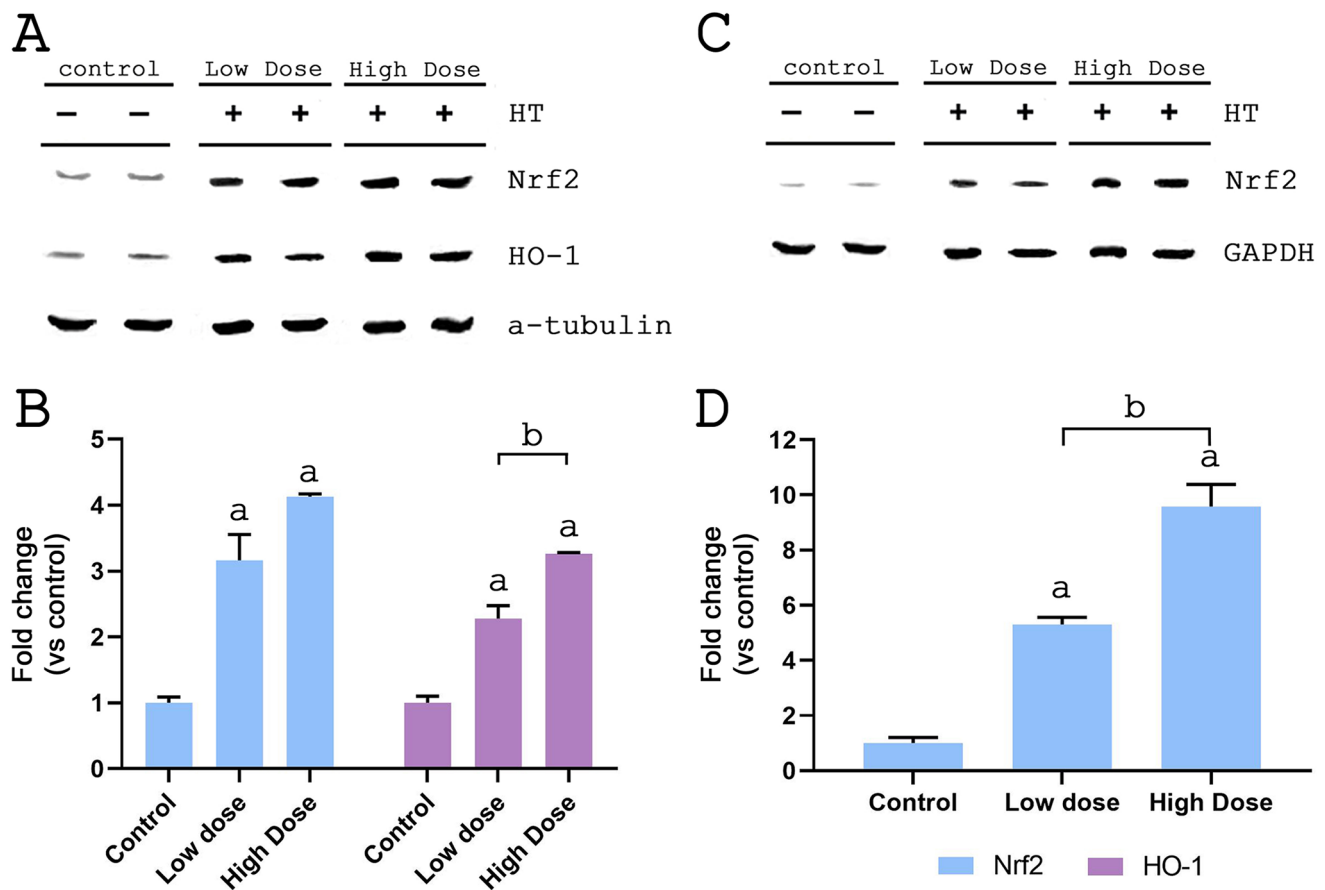


Figure 12. Supplementation with HT increases Nrf2 and HO-1 levels in hepatic protein extracts and induces Nrf2 translocation into nuclei. (A) Representative bands from total Nrf2 and HO-1 hepatic protein extracts. (B) Mice treated with a high dose of HT (25 mg/kg/day) exerted a significantly greater increase in total levels of HO-1 compared to the mice treated with the low dose (2.5 mg/kg/day). (C) Representative bands from nuclear Nrf2 hepatic protein extracts. (D) Mice treated with a high dose of HT (25 mg/kg/day) exerted a significantly greater increase in nuclear levels of Nrf2 compared to the mice treated with the low dose (2.5 mg/kg/day). The a-tubulin and GAPDH were used as the loading controls.

^aStatistically significantly different from control.

^bStatistically significantly different between groups. Data are presented as mean \pm standard deviation. All experiments were performed in triplicates.

in GSH levels (50%) and a minor one (13%) were seen in the low- and the high-dose groups of our *in vivo* experiment, respectively. GSH depletion could reflect increased levels of oxidation. Reports are pointing to the interpretation that decreased GSH concentrations are due to the conjugation of flavanols (such as catechin and epigallocatechin-3-gallate) to reduced GSH.^{38–40} Whether something similar applies to HT remains to be investigated.

In summary, we have shown that HT, a natural product of olive tree and its leaves as well as a by-product obtained from the manufacturing of olive oil, biosynthesized and purified to >95% purity, from genetically modified *E. coli* strains scavenges ROS *in vitro* by activating the Nrf2/HO-1 signaling pathway, thereby protecting cells against oxidative stress. The same positive effect of HT on the liver tissues of mice and the possible activation of the Nrf2/HO-1 signaling pathway with the potential release and translocation of Nrf2 to the nucleus was concluded, which seems to be following our *in vitro* research. Nonetheless, the mild increase in catalase activity and the decrease in GSH levels in mice plasma warrants further investigation to identify

a potential multifactorial effect of HT on the antioxidant network regulation.

AUTHORS' CONTRIBUTIONS

YVS and SZ contributed equally in the methodology, formal analysis, investigation, data curation, writing – original draft, and visualization of this article. PL contributed to the methodology and investigation. CZ was involved in the formal analysis and visualization. MH and FV contributed to the formal analysis, resources, supervision, and funding acquisition. EAT contributed to the formal analysis, resources, and data curation. KT contributed to the investigation and visualization. DP was involved in the formal analysis and data curation. CA contributed to the conceptualization, resources, and supervision. PV contributed to the conceptualization, resources, supervision, project administration, and funding acquisition.





DECLARATION OF CONFLICTING INTERESTS

The author(s) declared no potential conflicts of interest with respect to the research, authorship, and/or publication of this article.

FUNDING

The author(s) disclosed receipt of the following financial support for the research, authorship, and/or publication of this article: This work has been co-financed by the European Regional Development Fund of the European Union and Greek national funds through the Operational Program Competitiveness, Entrepreneurship and Innovation, under the call RESEARCH—CREATE—INNOVATE (project: T1EDK-04267).

ORCID IDS

Yannis V Simos  <https://orcid.org/0000-0003-1764-8906>
 Christianna Zachariou  <https://orcid.org/0000-0002-8032-4915>
 Filippos Ververidis  <https://orcid.org/0000-0002-3104-6103>
 Emmanouil A Trantas  <https://orcid.org/0000-0001-7536-101X>

REFERENCES

- Tejada S, Pinya S, del Mar Bibiloni M, Tur JA, Pons A, Sureda A. Cardioprotective effects of the polyphenol hydroxytyrosol from olive oil. *Curr Drug Targets* 2016;**18**:1477–86
- D'Angelo C, Franceschelli S, Quiles JL, Speranza L. Wide biological role of hydroxytyrosol: possible therapeutic and preventive properties in cardiovascular diseases. *Cells* 2020;**9**:1932
- Robles-Almazan M, Pulido-Moran M, Moreno-Fernandez J, Ramirez-Tortosa C, Rodriguez-Garcia C, Quiles JL, Ramirez-Tortosa MC. Hydroxytyrosol: bioavailability, toxicity, and clinical applications. *Food Res Int* 2018;**105**:654–67
- Agostoni C, Bresson JL, Fairweather-Tait S, Flynn A, Golly I, Korhonen H, Lagiou P, Løvik M, Marchelli R, Martin A, Moseley B, Neuhäuser-Berthold M, Przyrembel H, Salminen S, Sanz Y, Stain S, Strobel S, Tetens I, Tome D, van Loveren H, Verhagen H. Scientific Opinion on the substantiation of health claims related to polyphenols in olive and protection of LDL particles from oxidative damage (ID 1333, 1638, 1639, 1696, 2865), maintenance of normal blood HDL cholesterol concentrations (ID 1639), maintenance of normal blood pressure (ID 3781), “anti-inflammatory properties” (ID 1882), “contributes to the upper respiratory tract health” (ID 3468), “can help to maintain a normal function of gastrointestinal tract” (3779), and “contributes to body defences against external agents” (ID 3467) pursuant to Article 13(1) of Regulation (EC) No 1924/2006. *EFSA J* 2011;**9**:2033
- Beltrán G, Jiménez A, del Rio C, Sánchez S, Martínez L, Uceda M, Aguilera MP. Variability of vitamin E in virgin olive oil by agronomical and genetic factors. *J Food Compos Anal* 2010;**23**:633–9
- Romero C, Brenes M. Analysis of total contents of hydroxytyrosol and tyrosol in olive oils. *J Agric Food Chem* 2012;**60**:9017–22
- Bayram B, Esatbeyoglu T, Schulze N, Ozcelik B, Frank J, Rimbach G. Comprehensive analysis of polyphenols in 55 extra virgin olive oils by HPLC-ECD and their correlation with antioxidant activities. *Plant Foods Hum Nutr* 2012;**67**:326–36
- Britton J, Davis R, O'Connor KE. Chemical, physical and biotechnological approaches to the production of the potent antioxidant hydroxytyrosol. *Appl Microbiol Biotechnol* 2019;**103**:5957–74
- Trantas E, Navakoudis E, Pavlidis T, Nikou T, Halabalaki M, Skaltsounis L, Ververidis F. Dual pathway for metabolic engineering of *Escherichia coli* to produce the highly valuable hydroxytyrosol. *PLoS One* 2019;**14**:e0212243
- Deri-Zenaty B, Bachar S, Rebroš M, Fishman A. A coupled enzymatic reaction of tyrosinase and glucose dehydrogenase for the production of hydroxytyrosol. *Appl Microbiol Biotechnol* 2020;**104**:4945–55
- Chatzikonstantinou AV, Gkantzou E, Thomou E, Chalmpes N, Lyra KM, Kontogianni VG, Spyrou K, Patila M, Gournis D, Stamatis H. Enzymatic conversion of oleuropein to hydroxytyrosol using immobilized β -glucosidase on porous carbon cuboids. *Nanomaterials* 2019;**9**:1166
- Bouallagui Z, Sayadi S. Bioconversion of *p*-tyrosol into hydroxytyrosol under bench-scale fermentation. *Biomed Res Int* 2018; **2018**:7390751
- Allouche N, Sayadi S. Synthesis of hydroxytyrosol, 2-hydroxyphenylacetic acid, and 3-hydroxyphenylacetic acid by differential conversion of tyrosol isomers using *Serratia marcescens* strain. *J Agric Food Chem* 2005;**53**:6525–30
- Satoh Y, Tajima K, Munekata M, Keasling JD, Lee TS. Engineering of L-tyrosine oxidation in *Escherichia coli* and microbial production of hydroxytyrosol. *Metab Eng* 2012;**14**:603–10
- Chung D, Kim SY, Ahn JH. Production of three phenylethanoids, tyrosol, hydroxytyrosol, and salidroside, using plant genes expressing in *Escherichia coli*. *Sci Rep* 2017;**7**:2578
- Li X, Chen Z, Wu Y, Yan Y, Sun X, Yuan Q. Establishing an artificial pathway for efficient biosynthesis of hydroxytyrosol. *ACS Synth Biol* 2018;**7**:647–54
- Andersson HA, Arpaia S, Bartsch D, Casacuberta J, Davies H, du Jardin P, Flachowsky G, Herman L, Jones H, Kärenlampi S, Kiss J, Kleter G, Kuiper H, Messéan A, Magne Nielsen K, Perry J, Pöting A, Sweet J, Tebbe C, Johannes von Wright A, Wal J-M. Guidance on the risk assessment of genetically modified microorganisms and their products intended for food and feed use. *EFSA J* 2011;**9**:2193
- Xynos N, Abatis D, Argyropoulou A, Polychronopoulos P, Aliagiannis N, Skaltsounis AL. Development of a sustainable procedure for the recovery of hydroxytyrosol from table olive processing wastewater using adsorption resin technology and centrifugal partition chromatography. *Planta Med* 2015;**81**:1621–7
- Jansen EHJM, Beekhof PK, Cremers JWJM, Viezeliene D, Muzakova V, Skalicky J. Long-term stability of parameters of antioxidant status in human serum. *Free Radic Res* 2013;**47**:535–40
- Brinc D, Chan MK, Venner AA, Pasic MD, Colantonio D, Kyriakopoulou L, Adeli K. Long-term stability of biochemical markers in pediatric serum specimens stored at -80°C : a CALIPER Substudy. *Clin Biochem* 2012;**45**:816–26
- Roy UK, Nielsen BV, Milledge JJ. Effect of post-harvest conditions on antioxidant enzyme activity in *Dunaliella tertiolecta* biomass. *Biocatal Agric Biotechnol* 2020;**27**:101661
- Zerikiotis S, Angelidis C, Dhima I, Naka KK, Kasioumi P, Kalfakakou V, Peschos D, Vezyraki P. The increased expression of the inducible Hsp70 (HSP70A1A) in serum of patients with heart failure and its protective effect against the cardiotoxic agent doxorubicin. *Mol Cell Biochem* 2019;**455**:41–59
- Naka KK, Vezyraki P, Kalaitzakis A, Zerikiotis S, Michalis L, Angelidis C. Hsp70 regulates the doxorubicin-mediated heart failure in Hsp70-transgenic mice. *Cell Stress Chaperones* 2014;**19**:853–64
- Poudyal H, Lemonakis N, Efentakis P, Gikas E, Halabalaki M, Andreadou I, Skaltsounis L, Brown L. Hydroxytyrosol ameliorates metabolic, cardiovascular and liver changes in a rat model of diet-induced metabolic syndrome: pharmacological and metabolism-based investigation. *Pharmacol Res* 2017;**117**:32–45
- Andreadou I, Iliodromitis EK, Mikros E, Constantinou M, Agalias A, Magiatis P, Skaltsounis AL, Kamber E, Tsantili-Kakoulidou A, Kremastinos DT. The olive constituent oleuropein exhibits anti-ischemic, antioxidative, and hypolipidemic effects in anesthetized rabbits. *J Nutr* 2006;**136**:2213–9
- Marković AK, Torić J, Barbarić M, Brala CJ. Hydroxytyrosol, tyrosol and derivatives and their potential effects on human health. *Molecules* 2019;**24**:2001
- Hormozi M, Assaei R, Boroujeni MB. The effect of aloe vera on the expression of wound healing factors (TGF β 1 and bFGF) in mouse embryonic fibroblast cell: in vitro study. *Biomed Pharmacother* 2017;**88**: 610–6
- Hormozi M, Marzijerani AS, Baharvand P. Effects of hydroxytyrosol on expression of apoptotic genes and activity of antioxidant enzymes in LS180 cells. *Cancer Manag Res* 2020;**12**:7913–9
- An BC, Choi YD, Oh IJ, Kim JH, Park J-I, Lee S. GPx3-mediated redox signaling arrests the cell cycle and acts as a tumor suppressor in lung cancer cell lines. *PLoS One* 2018;**13**:e0204170
- Talalay P, Dinkova-Kostova AT, Holtzclaw WD. Importance of phase 2 gene regulation in protection against electrophile and reactive oxygen toxicity and carcinogenesis. *Adv Enzyme Regul* 2003;**43**:121–34

31. Zrelli H, Matsuoka M, Kitazaki S, Zarrouk M, Miyazaki H. Hydroxytyrosol reduces intracellular reactive oxygen species levels in vascular endothelial cells by upregulating catalase expression through the AMPK-FOXO3a pathway. *Eur J Pharmacol* 2011;**660**:275–82
32. Perrone MA, Gualtieri P, Gratteri S, Ali W, Sergi D, Muscoli S, Cammarano A, Bernardini S, Di Renzo L, Romeo F. Effects of postprandial hydroxytyrosol and derivatives on oxidation of LDL, cardiometabolic state and gene expression: a nutrigenomic approach for cardiovascular prevention. *J Cardiovasc Med* 2019;**20**:419–26
33. Valenzuela R, Echeverria F, Ortiz M, Rincón-Cervera MÁ, Espinosa A, Hernandez-Rodas MC, Illesca P, Valenzuela A, Videla LA. Hydroxytyrosol prevents reduction in liver activity of Δ -5 and Δ -6 desaturases, oxidative stress, and depletion in long chain polyunsaturated fatty acid content in different tissues of high-fat diet fed mice. *Lipids Health Dis* 2017;**16**:64
34. Pan S, Liu L, Pan H, Ma Y, Wang D, Kang K, Wang J, Sun B, Sun X, Jiang H. Protective effects of hydroxytyrosol on liver ischemia/reperfusion injury in mice. *Mol Nutr Food Res* 2013;**57**:1218–27
35. Aquilano K, Baldelli S, Ciriolo MR. Glutathione: new roles in redox signaling for an old antioxidant. *Front Pharmacol* 2014;**5**:196
36. Kouka P, Priftis A, Stagos D, Angelis A, Stathopoulos P, Xinos N, Skaltsounis AL, Mamoulakis C, Tsatsakis AM, Spandidos DA, Kouretas D. Assessment of the antioxidant activity of an olive oil total polyphenolic fraction and hydroxytyrosol from a Greek *Olea europaea* variety in endothelial cells and myoblasts. *Int J Mol Med* 2017;**40**:703–12
37. Vlavcheski F, Young M, Tsiani E. Antidiabetic effects of hydroxytyrosol: in vitro and in vivo evidence. *Antioxidants* 2019;**8**:188
38. Moridani MY, Scobie H, Salehi P, O'Brien PJ. Catechin metabolism: glutathione conjugate formation catalyzed by tyrosinase, peroxidase, and cytochrome P450. *Chem Res Toxicol* 2001;**14**:841–8
39. Galati G, Lin A, Sultan AM, O'Brien PJ. Cellular and in vivo hepatotoxicity caused by green tea phenolic acids and catechins. *Free Radic Biol Med* 2006;**40**:570–80
40. Sang IL, Hyo JK, Boo YC. Effect of green tea and (-)-epigallocatechin gallate on ethanol-induced toxicity in HepG2 cells. *Phytother Res* 2008;**22**:669–74

(Received October 25, 2022, Accepted June 5, 2023)